A high-pressure and high-temperature gas-loading system for the study of conventional to real industrial sized samples in catalysed gas/solid and liquid/solid reactions

Jérome Andrieux, Christophe Chabert, Anthony Mauro, Hugo Vitoux, Bernard Gorges, Thomas Buslaps, Veijo Honkimaki

A high pressure and high temperature gas loading system for the study of conventional to real industrial sized samples in catalyzed gas/solid and liquid/solid reactions

Jerome Andrieux [a,b*], Christophe Chabert [a], Anthony Mauro [a], Hugo Vitoux [a], Bernard Gorges [a], Thomas Buslaps [a] and Veijo Honkimäki [a]

[a] ESRF, ID15, European Synchrotron Radiation Facility, 6 rue Jules Horowitz, Grenoble, France, 38043, France

[b] Université Claude Bernard Lyon 1, LMI – UMR CNRS N° 5615, 43 Bd du 11 novembre 1918, 69622 Villeurbanne Cedex, France

Correspondence email: jerome.andrieux@univ-lyon1.fr

Keywords: Catalytic gas/solid and liquid/solid reaction; high energy X-ray; X-ray diffraction; hydrogen storage; high pressure; high temperature.

Synopsis

A high pressure-high temperature gas loading system has been developed for combined in situ high energy X-ray diffraction and mass spectrometry investigations during catalyzed gas/solid or liquid/solid reactions. The benefits of such a system are the combination of different gases, flexibility of the cell design and rotation of the cell with pressure, temperature and flow-rate values up to 200 bar, 1000°C and 1 $L.min^{-1}$, respectively. This opens up new opportunities for studying catalysts or compounds not just from a fundamental point of view but also for industrial applications, both cases in operando conditions.

Abstract

A high pressure-high temperature gas loading system (GLS) is described for combined in operando X-ray diffraction and mass spectrometry investigations during catalyzed gas/solid or liquid/solid reactions. The pressure cell consists of a single crystal sapphire tube which serves as both high pressure container and reaction cell up to 6mm inner diameter. The system can operate in two different configurations either under static high pressure or dynamic pressurized flow. The transportable reaction cell can be filled under inert atmosphere inside a glove box enabling studies

with oxygen-sensitive compounds to be conducted. The five main benefits of this system can be summarised as follows: i) the temperature, pressure and gas flow ranges of 25-1000°C, 10^{-3} mbar - 200 bar and 0-1 L.min^{-1}, respectively, ii) the combination of different gases, iii) the flexibility of the cell design, iv) the full rotation of the pressurized cell and v) the combination of X-ray diffraction and mass spectrometry as analytical tools. These five key points open new possibilities for studying catalysts or compounds evolutions from a fundamental point of view to industrial applications, both cases in operando conditions.

1. Introduction

The range of applications based on catalyzed reactions has grown steeply since the 1950s associated with extensive research on improving the kinetics and yield of chemical reactions. Nowadays, catalyzed reactions find applications in large-scale industrial development projects, such as car exhaust gas treatment, or in chemical and medicinal drug synthesis. In addition, the interest in green energy is the driving force behind, for example, recent studies in solid storage materials. A key point in improving the efficiency of catalyzed reactions is to determine which mechanisms are taking place during these reactions. Therefore, catalytic studies need to focus on both the characterization of the chemical changes in the catalyst and determination of the chemical pathway, i.e., consumption of reactants to form intermediate phases and finally the reaction products. This is of paramount interest in order to improve the efficiency and kinetics of a catalytic reaction.

It is well known that catalyst loading, particle size and distribution and specific surface are among the main parameters to be monitored and studied in the catalyst synthesis. Moreover, temperature and pressure are key parameters in catalyzed reactions as demonstrated, for example, in ethanol steam reforming (T = 700 °C and P = 11 bar), synthesis of ammonia from natural gas using Fe catalyst (T = 400-500 °C and P = 300 bar) or methanol synthesis from CO and H_2 using ZnO/Cr_2O_3 catalyst (T = 350-400 °C, P = 250-350 bar) (Spivey, 2010; Hagen, 2006). Although industrial applications exploit pressure to increase the efficiency of a catalytic reaction, fundamental research on catalytic mechanisms under pressure is still at an emerging stage.

In situ diffraction allows the crystallographic structural changes of crystallized compounds to be monitored during the course of a chemical reaction. The temporal resolution required for small quantities of different phases can be achieved using high brilliance synchrotron X-rays at 3rd generation synchrotron facilities. In addition, high energy X-ray radiation, such as that provided on the ID15 beamline at ESRF, can be used to work in transmission mode to obtain complex sample environments thanks to a deeper penetration depth.

Up to now, only a few systems have been built to carry out in situ synchrotron characterizations of gas/solid reactions under high pressure and high temperature, whereas the demand by a large scientific community is increasing (Clausen *et al.*, 1991; Chupas *et al.*, 2008; Jensen *et al.*, 2010; Wilkinson *et al.*, 2011). Two existing systems are based on a sapphire capillary design (inner diameter (ID) 1 mm, wall thickness (WT) 0.5 mm) and they are being used at the APS/Chicago and at MAX-II/Lund (Chupas *et al.*, 2008 and Jensen *et al.*, 2010 respectively). APS system can operate at pressures up to 300 bar on the temperature domain 300<T<973 K and for a maximum flow of 100 $ml.min^{-1}$. MAX-II system was designed to work under pressure up to ~138 bar and a wider temperature range from 80 K to ~1273 K. A third system, based on thin walled quartz or glass capillaries (P_{max} = 100 bar, temperature range 50<T<1273 K), is intensively used in static mode to study solid storage materials at the SNBL beamline (ESRF/Grenoble) (Jensen *et al.*, 2010). Based on Chupas & Jensen's cell design, other systems have been developed at ESRF, for example for EXAFS studies at ID24 (P_{max} = 20 bar, T_{max} = 1173 K, Figueroa *et al.*, 2013) and high resolution XRD studies at ID31 (P_{max} = 100 bar, Hill, 2013).

Regarding the specifications of the existing setups, the GLS described in this paper is unique. Its five main advantages can be summarised as follows:

i) the operational temperature, pressure and flow ranges of 25-1000°C, 10^{-3} mbar - 200 bar and 0-1 $L.min^{-1}$, respectively;

ii) the combination of different gases;

iii) the flexibility of the cell design (material, diameter, etc.);

iv) the full rotation of the pressurized cell;

v) and the combination of X-ray diffraction and mass spectrometry as analytical tools.

The following sections describe the design and give technical details of this high pressure – high temperature gas loading system. The main challenge was to develop a reaction cell with a high degree of versatility in size and design. A second challenge was the construction of a reaction cell to allow not just fundamental research studies to be carried out but also industry-oriented studies, both cases under in operando conditions.

2. Technical aspects

2.1. The reaction cell

The main component of the GLS is the reaction cell. This consists of a cylindrical tube which serves both as body and reaction cell. Among the different materials used to build the reaction cells, sapphire, Al_2O_3 (c.s. Trigonal, s.g. R -3 c), has been selected for its high ultimate tensile strength (theoretical ~ 2000 MPa, Dobrovinskaya *et al.*, 2009) and its chemical inertness. Sapphire can be used for high temperature studies involving highly corrosive, acid or basic compounds, like chemical hydrides for example. This is also one of the compounds which does not show any structural transition below 1000°C. Moreover, the distinctive diffraction signal of this single crystal helps to identify the powder diffraction pattern arising from the sample. Sapphire single crystal tubes were grown by the Chokralsky method with the [0001] direction parallel to the axis of the tube. The crystal tubes were supplied by Crytur (http://www.crytur.cz) with an as-grown inner and outer surface finish. An additional important asset of the cell is its transparency to the scientist's eye facilitating sample preparation and cell filling. Moreover, such a cell is not only transparent to high energy X-ray and visible light, but also to UV and IR (Dobrovinskaya *et al.*, 2009). This property allows auxiliary analysis techniques to be used, combining XRD with Raman/IR spectroscopic techniques for example.

The maximum pressure, P_{max}, that the wall can withstand in the direction perpendicular to the axis of the cylinder without failing was calculated according to Von Mises criteria (Arnold *et al.*, 2003) for an ideal cylindrical vessel under uniform pressure and is a function of the ultimate tensile strength, τ, of the chosen material and the ratio between the outer (d_o) and inner (d_i) diameters of the vessel. It can be approximated by eq.1.

$$P_{\max} = 2\tau \ln\left(\frac{d_o}{d_i}\right) \qquad \text{Eq.1}$$

For a given value of P_{max}, increasing the inner diameter of the cell requires an increase in the wall thickness (WT). The wall thickness was as a consequence chosen to withstand a maximum pressure higher than 200 bars, satisfying eq.1, given the variation of the inner diameter from 1 to 6mm.

Three main standard sapphire cells are currently available, as illustrated on Figure 1. The first (Figure 1.a) was used for most of the experiments carried out using the GLS. It is based on a sapphire tube with an inner diameter of 3.0 mm and a wall thickness of 0.5 mm (tolerance ± 0.1 mm). An inner diameter of 3.0 mm was selected to provide enough material to interact with high energy X-rays in the case of weakly diffracting samples, i.e. light elements, such as chemical hydrides. It also leads to sample averaging while maintaining an acceptable resolution with respect to the ID15 beamline configuration. The second cell (Figure 1.b) was dedicated to experiments requiring better angular resolution or to samples containing highly absorbing elements. Sapphire cell dimensions were ID = 1 mm and WT = 0.5 mm. A large dimension cell (ID = 6 mm, WT = 1 mm) was designed for studying "real size" industrial samples such as catalyst pellets (Figure 1.c). Note that the wall thickness up to 1 mm is still sufficiently small for auxiliary spectroscopy studies with high numerical aperture optics, at least to characterize the sample just below the wall (Raber *et al.*, 2006). Finally, the cell size can be adapted in diameter, wall thickness, length and nature of cell materials to fit user requirements, illustrating the high versatility of the cell design.

Figure 1. Examples of different cells developed for the GLS. a) standard cell (ID 3 mm, WT 0.5 mm) and details of the mechanical connection (inset), b) high resolution cell (ID 1 mm, WT 0.5 mm), c) in operando cell (ID 6 mm, WT 1 mm) and details of the bonding connection (inset).

It is worth pointing out that, like the cell developed at SNBL (Jensen *et al.*, 2010), the safety factor for the maximum pressure is a matter of local regulations. The reaction cells were designed to be used up to 200 bar working pressure (the maximum internal pressure of gas bottles). The effective ultimate tensile strength lies, in the case of sapphire tube, in the range 60-120 MPa depending on the degree of

machining and annealing, which is approximately 20 times less than the theoretical value (~2000 MPa, Dobrovinskaya *et al.*, 2009). Taking into account this tensile strength range and according to eq.1, a burst pressure range of 350-700 bar is predicted, given the dimensions of the three cells described above. This suggests that a maximum working pressure of 200 bar should be acceptable in a research situation, with a safety factor varying from 1.75 to 3.5. Moreover, calculations based on eq. 1 are valid at room temperature. The ultimate tensile strength might decrease at higher temperature but no data are available in the literature to the authors' knowledge. Thanks to the large safety factor, as is the case in our cells, studies can be performed in safe conditions even, for example, at 200 bar and 1000°C. In addition, each tube was tested at the maximum temperature needed by the experiment and at 200 bar. More than 96% of the sapphire tubes successfully passed these pressure tests. Failure of the other sapphire tubes could possibly be explained by residual defects or mechanical stresses induced by the sealing.

2.1.1. Connection of the reaction cell to the gas lines

The reaction cell, i.e. the sapphire tube, has to be connected to the gas lines. In order to be able to use a wide range of cell sizes, two different kinds of connection were developed.

Firstly, a mechanical tightening system was used mainly to connect the sapphire tube to the gas lines as illustrated on Figure 1.a and b. In this case, a conventional ¼" VCR to ¼" Swag fitting (SS-4-VCR-6-400, Swagelok, France) was used. This technique was chosen for its rapidity and flexibility. It also enables the sapphire tube to be dismantled from the fitting after an experiment, facilitates the cleaning of the tube and the reuse of the elements (fittings and tubes) for other experiments. The assembly was sealed using Vespel® ferrules, as developed for other systems (Jensen *et al.*, 2010). Holes defining the inner diameter were drilled on blind Vespel® ferrules supplied by Analytical Columns (www.analyticalcolumns.com). In this way, the mechanical tightening system can be adapted for tubes with outer diameter varying from 2 to 6 mm. Vespel® polymer (polyimide-based plastics) was selected among other materials for its elasticity and its working temperature range, up to 300°C.

In the case of sapphire tubes with big outer diameter (i.e., 8 mm as in the in operando cell), the sapphire tube was glued to a metal fitting as illustrated in the inset of Figure 1.c. It is quite an easy technique to join ceramic to metal and it is used on other systems (Chupas *et al.*, 2008; Jensen *et al.*, 2010). However, the two major drawbacks were the irreversibility of the assembly and the difficulty of aligning the tubes with the fittings. The sapphire tube was bonded to the metal fitting using dual-

component epoxy glue (E707) supplied by Epotecny (www.epotecny.com). This glue was cured at 150°C for 1 h. The maximum working temperature of this glue is 300-350°C.

These connection techniques, mechanical tightening or bonding, were able to withstand 200 bar and 1000°C applied on the cell. Note that the sealing temperature is much lower than the temperature of the sample located ~5 cm from the seal.

Regardless of the type of connection, mechanical tightening or bonding, the fitting has to be attached to a ¼" VCR cross for gas connections. Two possibilities exist depending on the nature of the compounds to be studied. For non oxygen/moisture sensitive compounds, the easiest way is to use a rotary female union (as illustrated in the inset of Figure 2.a.). For oxygen/moisture sensitive compounds, a manual valve (6LVV-DPHFR4-P, Swagelok, France) is used as illustrated in Figure 2.a: the cell can be filled with the sample under inert atmosphere and then connected to the gas lines, the manual valve being closed. The whole assembly, including the sapphire tube, the metal fitting and the manual valve (or the rotary female union), is called "cell" or "reaction cell" in the present paper.

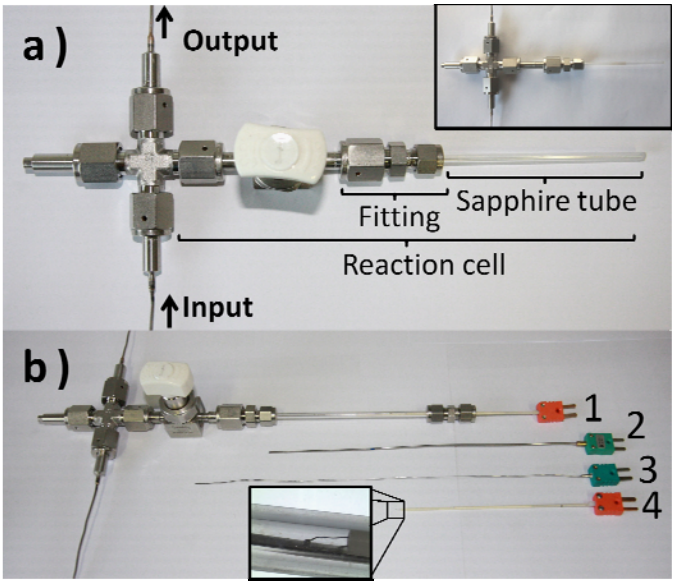

Figure 2. a) reaction cell in high pressure configuration (config. A) using a manual valve or VCR straight union (inset), b) details of thermocouple connections for config. A (1. thin-wire S type thermocouple, 2. sheathed Ø 1.5 mm K type thermocouple, 3. sheathed Ø 0.5 mm K type thermocouple, 4. same thermocouple as in Figure 2.b-1 and details of a thin-wire S type thermocouple spot-welded to a sample and placed inside the cell (inset)).

2.1.2. High pressure and high flow configurations

Two configurations are available to carry out experiments. The first, called “high pressure configuration” or “Config. A”, was used for static pressure experiments. The sapphire tube is closed at one end (closed by the supplier) (Figure 2.a). Pressure can be applied on the sample in static or dynamic mode as discussed below (see Section 3.2). Note that a gas flow can also be injected from the top of the tube. This provides an inert atmosphere over the sample or carries away the gases released during a chemical reaction via a carrier gas. The sample temperature can be measured by two different approaches. The first method uses “sheathed” thermocouples of different diameter to measure the temperature of a powder sample for example (Figure 2.b-2 and 2.b-3). The second is based on a “thin-wire” thermocouple placed inside a double bore alumina rod (Figure 2.b-1 and 2.b-4). This thermocouple can be spot-welded to a solid sample (cf. inset of Figure 2.b-4).

A second configuration, called “high flow configuration” or “Config.B”, was used for dynamic experiments where both flow and pressure can be applied (Figure 3.a). In this case, the second end of the tube was connected to a VCR tee with the same connection techniques as those described above (mechanical tightening or bonding). In this case, the gas flow was injected through the sample. The third connection of the VCR tee can be used to insert a thermocouple in the cell as illustrated in Figure 3.b. Like config. A, two kinds of thermocouple were used: “sheathed” or “thin-wire” thermocouples (Figure 3.b).

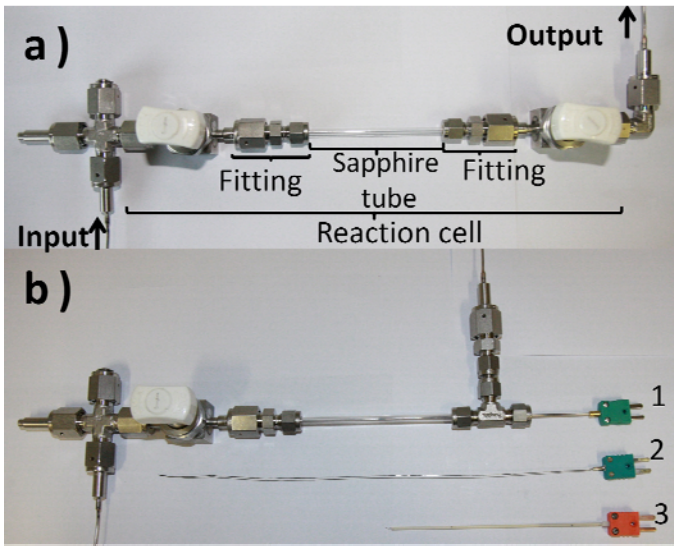

Figure 3. a) reaction cell in high flow configuration (config. B), b) Details of thermocouple connections for config. B (1. sheathed Ø 1.5 mm K type thermocouple, 2. sheathed Ø 0.5 mm K type thermocouple, 3. thin-wire S type thermocouple).

For both config. A and B, thermocouples (K or S type) can be used up to 1000°C and 200 bar via a mechanical connection. The sample temperature can be read and recorded during the course of a reaction and simultaneously with XRD acquisitions thanks to the use of an electronic interface (Wago box, www.wago.com) connected to SPEC software.

The fourth connection of the VCR cross was connected to a goniometer head (1003, Hubert, Germany) via a modified VCR fitting (SS-4-VCR-3-BL, Swagelok, France) as illustrated in Figure 4. In this way, the cell can be manually aligned under the beam. In both configurations, the reaction cell was always placed vertically. As a consequence, the X-ray beam impacted the cell in a direction perpendicular to the longest axis of the tube and experiments were performed in transmission mode. Figure 4 presents a general view of the cell installed on the goniometer head and the associated degrees of freedom allowing cell alignment and rotation. This mounting method allows working with liquid phases and decreasing the force applied to the goniometer head holding the cell, thereby improving the position precision.

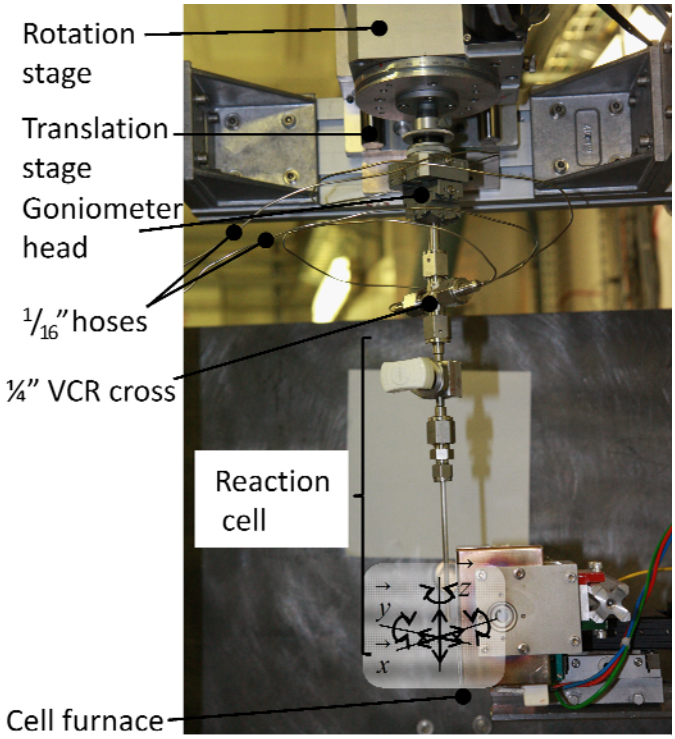

Figure 4. General view of the reaction cell installed on the goniometer head and associated degrees of freedom.

For both config. A and B, the reaction cell was connected to the gas lines via stainless steel 1/16" hoses (SS-T1-5-014-6MF, Swagelok, France) as illustrated on Figure 4. The stainless steel hoses were connected to the gas lines using VCR fittings (SS-4-VCR-3-2MTW, Swagelok, France). This mounting system allows the gas to flow over (Figure 2.a) or through (Figure 3.a) the cell and the application of high pressure on the sample. In these conditions, once the reaction cell was connected to the gas lines via the hoses, it can be considered to be a closed system and different vacuum/argon purges can be implemented. Thanks to the flexibility of the 1/16" stainless steel hoses, the cell can be rotated under high pressure and temperature. A maximum rotation angle of 270° and a maximum rotation speed of $30°.s^{-1}$ were achieved in both config. A and B using a rotation stage (409-10037, Hubert, Germany). In addition, the rotation stage holding the cell was fixed to a translation stage (5101.20, Hubert, Germany) in order to adjust the height of the sample with respect to the beam (Figure 4).

2.2. The gas lines

The GLS includes two gas lines. The first, called "gas distribution line" (Figure 5), is used to select different kinds of gases, connecting the reaction cell to vacuum or releasing the gas to an exhaust line under high pressure conditions. The second, called "evacuation line" (Figure 6) links the output of the reaction cell to the low pressure exhaust. Both gas lines were equipped with remote controlled pneumatic valves (6LVV-DPHFR4-P-C, Swagelok, France) and can be used up to 250 bar according to the supplier's data. Pneumatic valves were open or closed by 7 bar of compressed air via solenoid valves, controlled by an electronic interface (Wago box, www.wago.com) connected to SPEC software. The remote control of the pneumatic valves allows a high pressure, gas flow or vacuum to be applied according to the desired experimental configuration. Note that the different parts of the system ("gas distribution line", reaction cell and "evacuation line") can be isolated. The different experimental configurations (high pressure, gas flow or vacuum) can be selected and changed during the course of an experiment, authorizing cycling studies, for example, as illustrated in Section 4.

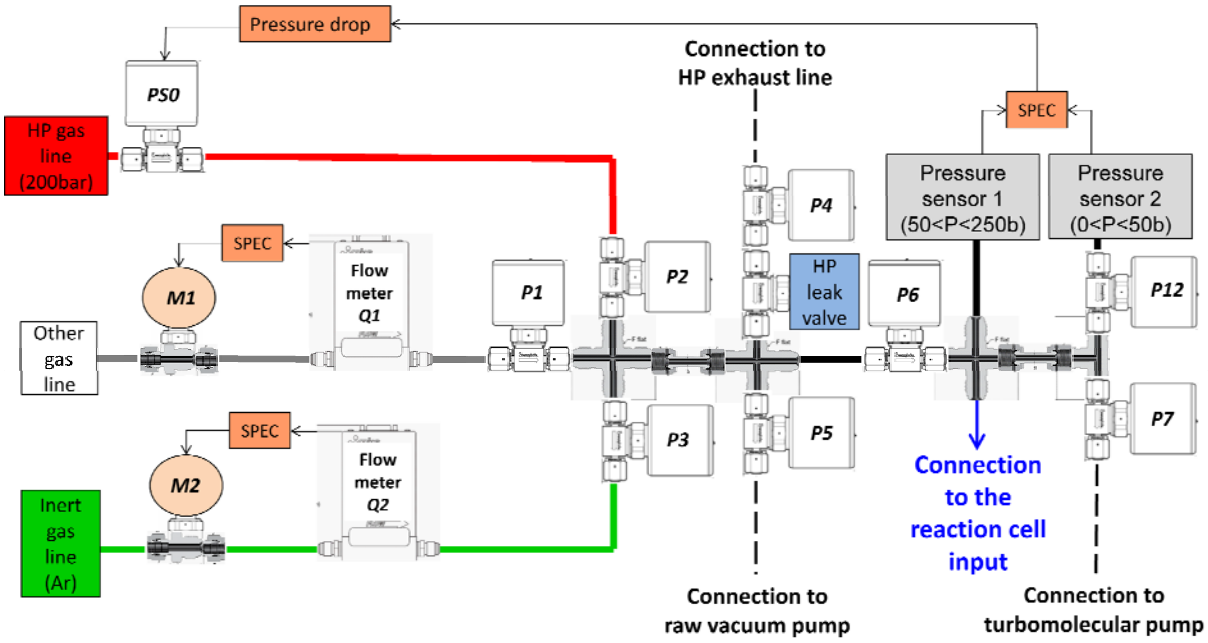

Figure 5. General diagram of the "gas distribution line". HP = High Pressure.

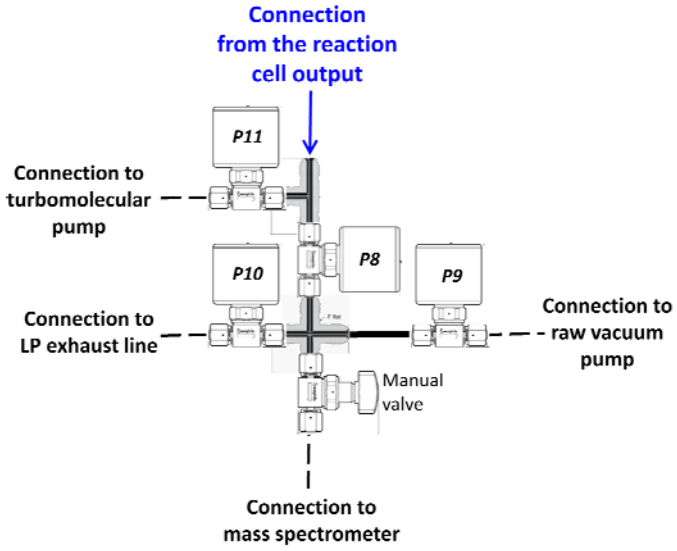

Figure 6. General diagram of the "evacuation line". LP = Low Pressure.

Depending on the experimental configurations, different items can be fitted to or removed from the "gas distribution line". For example, working under high pressure and flow, high pressure mass flow controllers (EL-FLOW F230M, Bronkhorst, Netherlands) can be used. Working under ambient pressure and flow, a leak valve (SS-SS4, Swagelok, France), modified to be motorized and controlled by a flow meter (179B, MKS, USA), defines the desired flow (*M1* and *M2* on Figure 5). In these cases, two different flow meters can be used on the system: one with a 0-100 $ml.min^{-1}$ flow range (calibrated for hydrogen) and one with a 0-1000 $ml.min^{-1}$ flow range (calibrated for argon). Under ambient pressure, the maximum working flow (argon) over the cell (Config. A), and through the cell (Config. B), was measured at 1000 $ml.min^{-1}$, meaning that gas flow was not restricted by the 1/16"

stainless steel hoses (at least in the flow range of the argon mass flow meter). The flow rate of gases can be read and recorded during the course of a reaction simultaneously with XRD acquisitions thanks to the use of an electronic interface (Wago box, www.wago.com) connected to SPEC software.

The "gas distribution line" configuration presented on Figure 5 corresponds to the set-up used for hydrogen storage experiments: one line was used for applying high hydrogen pressure. This gas line can be isolated by closing pneumatic valve *P2*. Another gas line was dedicated to working under argon flow (isolated by *P3*). The third gas line is a spare line for working under pressure or with a gas other than Ar and H_2 (isolated by pneumatic valve *P1*). Note that the gas line configurations of the GLS can be adapted to meet to the user's needs. The reaction cell was supplied with the selected gas by opening pneumatic valve *P6*, where the input of the reaction cell was connected. For a high pressure experiment, pneumatic valve *P4* then connects the "gas distribution line" to a high pressure exhaust line which is equipped with a manual high pressure leak valve (Millimite Hoke valve, 240-0.02, Air Liquide, France) to select the leak rate (controlled decrease in cell pressure from ~0.003 to ~60 $bar.s^{-1}$). In addition, the "gas distribution line" is connected to vacuum via pneumatic valves *P5* (primary pump) and *P7* (turbomolecular pump). Finally, two pressure sensors can be used depending on the pressure range: sensor 1 is used for $50 < P < 250$ bar (precision: 0.5 % FS, PTI-E-AG250, Swagelok, France) whereas sensor 2 is used for $1 < P < 50$ bar (precision: 0.01 % FS, PR 33X, Keller, Switzerland). The working pressure sensor was automatically selected in relation to the working pressure. The pressure applied on the sample can be read and recorded during the course of a reaction at the same time as XRD acquisitions thanks to the use of an electronic interface (Wago box, www.wago.com) connected to SPEC software.

Note that working under high flow and pressure (Config. B), a pressure regulator (EL-FLOW, F-033C, Bronkhorst, Netherlands) can be installed at the output of the reaction cell. Otherwise, the output of the reaction cell is connected via pneumatic valve *P8* to the "evacuation line" (Figure 6). Opening pneumatic valve *P10* connects the output of the reaction cell to a low pressure exhaust line. A T-branch, installed between *P8* and *P10*, allows a mass spectrometer to be connected via a manual valve (Figure 6). In addition, the "evacuation line" is connected to vacuum via pneumatic valves *P9* (primary pump) and *P11* (turbomolecular pump).

2.3. Cell furnace

The temperature range that can be obtained in the system is from 25°C (298 K) to 1000°C (1273 K). To heat the cell from room temperature up to 1000°C, several furnaces were investigated (gas blower, cylindrical furnace, infrared lamps) but none of them met the requirements of such a system and experiments, i.e., a cell outer diameter from 2 to 8 mm, a higher temperature profile and possibility of heating the reaction cell in both config. A and B. First, a homogeneous temperature zone along the

reaction cell had to be obtained to heat a greater sample volume in order to obtain a higher quantity of released gases. As these gases were carried away to a mass spectrometer via a carrier gas (argon), the higher the volume of gases released, the higher the concentration of the released gas in the carrier gas, leading to an increase in the signal-to-background ratio for gas detection. Second, the maximum wall thickness of the sapphire tube was 1 mm (i.e., for the in operando cell, Figure 1.c). Given the thermal conductivity of sapphire (~ 45 $W.m^{-1}.°C^{-1}$), a high thermal power was required to heat the sample in the cell to a maximum temperature of 1000 °C.

These requirements were met by using a home-made furnace (Figure 7.a and c), based on two heater holders (machined alumina plates). On both holders, U-shaped spiral heaters (Fe-Ni-Cr kanthal wires resistant to air oxidation) ensure symmetrical heating of the cell (Figure 7.b and d). The distance between the two heater holders was 10 mm. A sheathed Ø 0.5 mm K type thermocouple, placed inside the furnace close to the heater (Figure 7.b), was used to measure the furnace temperature (F_{temp}). A hole (inlet hole diam = 2 mm, outlet hole diam = 10 mm) was drilled perpendicular to the ceramic plates to allow the X-ray beam to go through (Figure 7.b). An opening window of ~ 40° allows the diffracted X-ray beam to be collected. Thermal shielding (quartz wool) was then placed between the heater holders and the metal covers to limit heat losses. The metal cover (Figure 7.d) can be removed to insert the reaction cells built in config. B. The furnace was placed on a set of manual (X and Z axes) and motorised (Y axis) translation stages so that it can be positioned with respect to the cell, aligned in the beam and moved in or out.

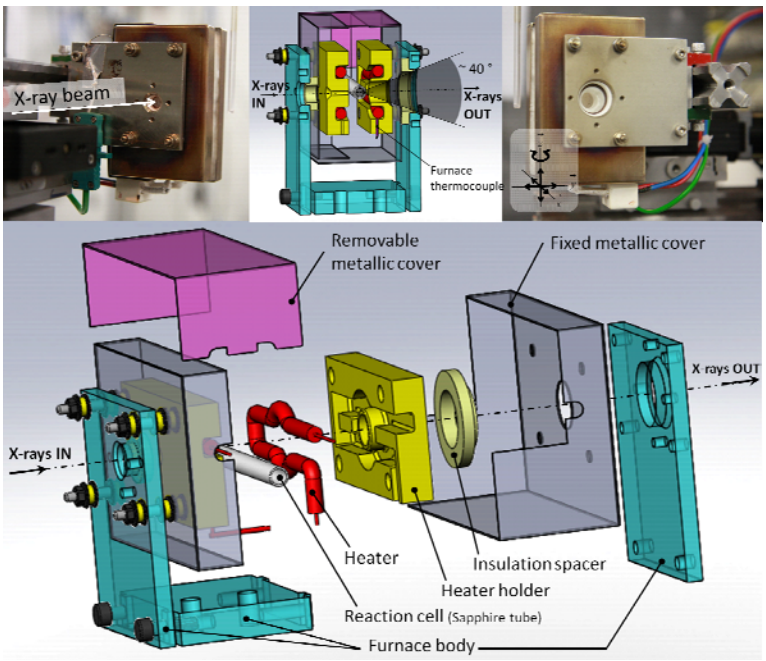

Figure 7. Cell furnace developed for the GLS. a) front view photograph. b) 3D cross section in the plane of the X-ray beam and the sample. c) rear view photograph where the degrees of freedom of the furnace are indicated. d) 3D 'exploded' view. The empty spaces between the heater holders and the metal covers are filled with heat shielding (compressed quartz wool).

In order to calibrate the temperature profile along the cell, the sample temperature (S_{temp}) was obtained using a sheathed Ø 1.0 mm K type thermocouple placed inside the sapphire tube in config.A (see Figure 2.b-2). The temperature profile was calibrated using a standard sapphire tube (ID 3 mm, WT 0.5 mm) and an argon flow over the tube of 500 mL.min^{-1} (P = 2 bar).

The temperature profile along the cell is shown on Figure 8. Measurements were repeated 3 times for each temperature. As expected, the first observation was a temperature gradient along the reaction cell. While the temperature is around 900°C in the beam position, the temperature at the edges of the furnace falls to ~ 300°C (Max position = 45 mm). However, the main result is that an off-centred temperature homogeneity zone of 25 mm was obtained with a maximum deviation of ± 7 °C in the temperature range 25-900°C (Figure 8 and Table 1). Thus, according to Table 1, the temperature deviation is of ± 5°C if the temperature profile is centred on the beam position to within ± 10 mm. These results demonstrate above all an excellent temperature stability and precision in the sample volume probed by the X-ray beam. They also show that a sample length/height of about 10 mm can be used to increase the volume of gases released, considering a ΔT of ± 5 °C to be acceptable in the experimental configuration.

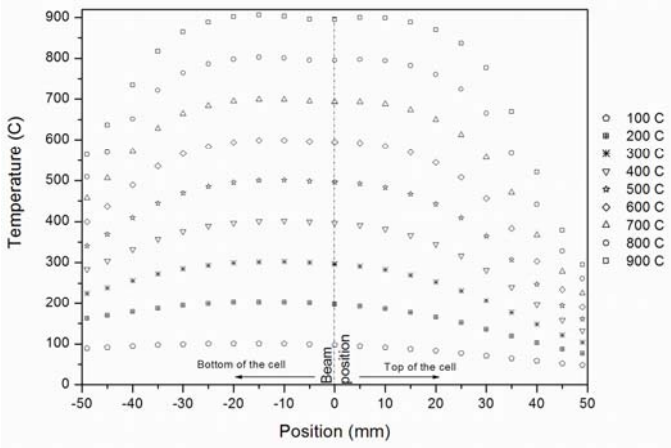

Figure 8. Temperature profile along the cell as a function of sample temperature (100-900°C). Sample temperature was measured using a sheathed Ø 1.0 mm K type thermocouple in config. A (see Figure 2.b-2). The position '0' of the thermocouple is the beam position. The displacement of the thermocouple inside the cell was ± 45 mm, defining a temperature profile over 90 mm, i.e., the furnace length. Tests performed using a standard sapphire tube (ID 3 mm, WT 0.5 mm).

Table 1. Average temperatures and deviations calculated from the temperature profiles presented on Figure 8.

Sample setpoint at '0' position (°C)	Centered on beam 10 mm (-5 to +5)		Off-centered 15 mm (-10 to +5)		Off-centered 25 mm (-20 to +5)	
	Av. temp (°C)	ΔT (°C)	Av. temp (°C)	ΔT (°C)	Av. temp (°C)	ΔT (°C)
100	97	2	98	3	99	4
200	197	4	198	5	199	7
300	296	5	297	5	298	7
400	396	5	398	5	398	6
500	496	4	497	5	497	5
600	594	2	596	4	596	4
700	694	2	695	4	696	4
800	796	2	797	4	798	5
900	897	3	899	5	900	6

3. General considerations using the GLS

3.1. Safety considerations

Special safety rules must be followed when experiments are carried out under dynamic conditions and high pressure, using a flammable gas (i.e., H_2, CO). Indeed, the cell has to stay connected to the gas bottles throughout the experiment (dynamic condition). For this purpose, the flammable gas line is equipped with *PS0*, also called "safety valve". Consequently, a program reads the cell pressure value every 500 ms and runs in parallel with the acquisition and temperature programs. If a pressure drop occurs, pneumatic valves *PS0*, *P2* and *P6* are automatically closed within 1 s: gas lines are closed and the reaction cell is isolated from the rest of the system. The first consequence of this arrangement is that samples can be protected from contamination in case of an empty bottle or physical problem on the gas lines, for example. The second, and more important, consequence is a reduction in the quantity of flammable gas released in the hutch in the event of a reaction cell failure. Given the volume of the reaction cell and hose from *P6* to *P8* (i.e., 23.432 cm^3 at room temperature), the maximum volume of gas released to the atmosphere after a cell failure at 200 bar equals ~ 5 L. If the gas released is, for example, pure hydrogen, given the volume of air in the ID15 experimental hutch, conditions are well below the lower explosive limit for H_2 (i.e., 4 %).

3.2. Experimental considerations

Experiments can be run according to five different approaches related to user needs. First, experiments can be performed under real static conditions: the reactor cell is loaded with an initial pressure P_0 and then isolated from the gas lines: the pressure will decrease or increase according to the reaction studied. In this case, pneumatic valve *P6* is closed after cell loading (*P8* valve being closed to apply a static pressure). As the volume between *P6* and *P8*, containing the reaction cell, has been calibrated (i.e., 23.432 cm^3 at room temperature), the pressure variation during an experiment can be related to the quantity of hydrogen released or absorbed. This configuration can also be used, for example, for solvothermal synthesis studies. Second, experiments can be carried out under pseudo-static conditions: the reactor cell is loaded with an initial pressure P_0 and, during the course of an experiment, the pressure is kept constant ($P \sim P_0 = constant$) by leaving the reactor connected to the gas line ($V_{cap} << V_{gasline}$). In this case, *P8* is closed but *P6* remains open. This configuration was used, for example, for the hydrogenation study of the $LiH+MgB_2$ mixture (Section 4). Special consideration must be given to the temperature increase in this second approach. During an experiment, as the temperature increases, the pressure in the reaction cell will increase. To compensate for this temperature increase, a program regulates the pressure at a given setpoint by opening or closing *P4* (high pressure exhaust line). The high pressure leak valve is adjusted in relation to the desired leak rate. Third, the pressure can be changed during the experiment from 10^{-3} mbar to 200 bar (dynamic conditions). This configuration was used, for example, for the cycling study of nanoconfined palladium nanoparticles (Section 4). Fourth, a gas flow can be applied over or through the sample and can be changed during the experiment from 0 to 1 $L.min^{-1}$ (dynamic conditions). Fifth, the combination of the last two approaches allows working under pressurized flow, and both gas pressure and flow can be changed during the experiment.

3.3. Sample preparation and handling

The main advantage of a single crystal sapphire is its chemical inertness, meaning that the tubes can be reused for different experiments. After mechanically cleaning the tubes to remove most of the previous sample, they were chemically cleaned with nitric acid under sonication and dried at 150°C. The next step was to connect the tube to the metal fitting to prepare a reaction cell (as illustrated in Figure 2.a).

The cell was aligned perpendicular to the beam before the beginning of an experiment using the goniometer head holding the cell. The alignment procedure also places the cell coaxial to the axis of rotation of the rotation stage which has two consequences. First, the cell can rotate to meet the needs of an experiment. Second, different cells were always placed in the same position compared to the

detector, i.e., the sample-detector distance stayed the same even if different cells and samples were used. After alignment, the cell was inserted in the furnace and the experimental hutch was closed.

A key requirement when working with moisture sensitive compounds, such as borohydrides, or oxygen sensitive compounds, such as metal nanoparticles, is to reduce the oxygen and moisture level in the gas lines. For this purpose, the tube of the reaction cell was firstly heat-treated at 600°C for 3 hours under secondary vacuum by connecting the cell directly to a turbomolecular pump. Once the manual valve was closed, the cell was ready to be placed in a glove box. Under inert atmosphere, the cell was filled with the sample, and the manual valve was closed. The cell was then connected to the GLS on the VCR cross as illustrated in Figure 4. After connection, the gas lines can be repeatedly evacuated, argon flushed and even pressurized. Purge cycling also allows a leak test on the gas connections to be performed. After 10 argon/vacuum purges and after leak testing of the gas line connections, the manual valve was opened in argon flow mode (P = 2 bar). A final pressure test was performed, with the manual valve open, in order to leak-test the connection of the sapphire tube to the metal fitting (mechanical tightening or bonding). Note that, thanks to the choice of stainless steel as material for the gas lines, valves and hoses, the entire GLS could be back-out (using heating elements or blowing hot gas) during the purge procedure, reducing the oxygen and moisture content even further. The reaction cell was then connected to a turbomolecular pump (by opening the pneumatic valves *P7* and *P11*). An additional vacuum step from 30 min to several hours ensured a minimum level of O_2/H_2O in the gas lines. Finally, after the purge procedure, the sample and the gas line were placed in the initial conditions of the experiment (vacuum, argon flow or hydrogen pressure).

Since the cell consists of a single crystal sapphire tube, strong diffraction spots were collected at the same time as the sample information. For small X-ray energy values, a simple rotation of the cell by a few degrees can prevent Bragg diffraction conditions (Jensen *et al.*, 2010). However, for high energy X-ray beams, the Ewald sphere is larger and it was not possible to find an angular position without diffraction conditions. To overcome this problem, a lead mask was placed in the front of the detector to absorb the diffraction signals from the sapphire tube. It is made of a Plexiglas plate where lead pieces are fixed. The lead pieces positions correspond to the diffraction spot positions of the single crystal sapphire tube.The use of a lead mask had the advantage of avoiding any damage to the detector. In addition, as diffraction spots from the sapphire cell were removed by the lead mask, detector parameters (gain and exposure) were maximized to detect phases in small quantity.

3.4. Data analysis

For the data analysis procedure, Figure 9.a can be considered as a raw image. It contains both information from the sample (diffraction rings) and the contribution of the lead mask (darker area). Starting from the raw image, the first step in the data analysis was to correct from 2D flat panel artefacts on the intensity (geometrical correction, spreading of diffraction spots on several pixels as a function of 2 theta and response of different detector sectors, Figure 9.b). In addition, the images were corrected from the polarization of the synchrotron X-ray beam and normalized by the incoming flux of photons. The resulting image (Figure 9.b) still contained some darker areas due to the lead mask. The next step of the data analysis was to apply a numerical mask to ignore the area of the image related to the lead mask (Figure 9.c). Note that even if part of the detector area was numerically masked, ~70 % of the detector area was still available for collecting sample information. The final step of the data analysis involved radial integration which converts the 2D image containing the diffraction rings from the sample into a 1D diffractogram (I=f(2Theta), Figure 9.d). This data analysis procedure was then implemented in a Matlab® script in order to analyse the entire dataset containing several files. The final results were text files ready to be used for Rietveld refinement. In addition, diffractograms can be plotted as a function of time or temperature as illustrated in the following section.

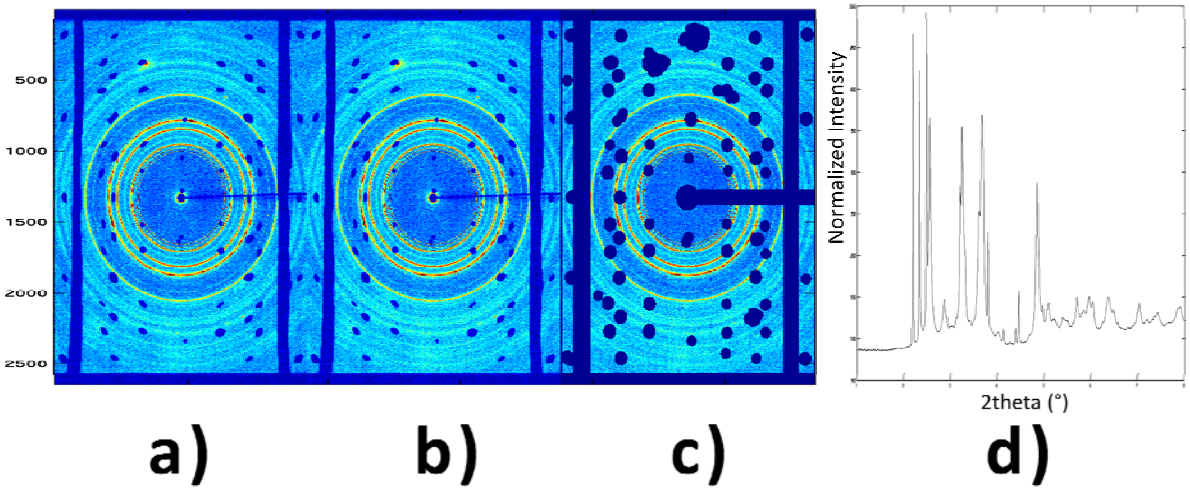

Figure 9. Steps of the data analysis procedure. a) raw image, b) resulting image after detector and beam corrections, c) resulting image after masking the lead mask contribution, d) resulting diffractogram after radial integration.

4. Application fields of the GLS

Due to the recent development of the gas loading system, the following examples will be described briefly to demonstrate the experimental feasibility using this system and its application fields. Further results and details will be given in future related papers.

Experiments were carried out on the ID15B beamline in transmission and monochromatic mode (E = 90 keV, λ = 0.1377 Å). Vacuum tubes were used on the upstream side and a tungsten beamstop was placed on the downstream side to minimize the air scattering effect. The diffraction rings were collected using 2D flat panel detectors protected by a lead screen. Depending on the time resolution required, either PIXIUM 4700 or MAR345 detectors were used (Daniels & Drakopoulos, 2009) and the sample-detector distance was about 1300 mm.

The GLS can be used to follow the phase changes under high temperature and pressure of microscopic grain size polycrystalline samples. The example given on Figure 10.a involves a reactive hydride composite (RHC, $LiBH_4$+MgH_2) heated from RT to 520 °C @ 5 °C.min^{-1} under an inert atmosphere (Ar) in config. A (*Courtesy of L. Laversenne, Institut Néel, Grenoble*). Transformations such as structural transitions (Step 1: $LiBH_4(\alpha)$→$LiBH_4(\beta)$), melting (Step 2: $LiBH_4(\beta)$→Liq.) and hydrogen desorption (Step 3: MgH_2→Mg+H_2) were followed in terms of phase identification, quantification and reaction kinetics. The same kind of transformations (Step 1: phase formation; Steps 2 and 4: structural transition), together with crystallization and in situ chemical reaction (Step 3: 2LiH + MgB_2 + 4H_2 → 2$LiBH_4$ (β)+ MgH_2), were also monitored on cooling (400°C to RT) under 100 bar of H_2 pressure during the hydrogenation of a LiH and MgB_2 mixture (Figure 10.b). The use of low background single crystal sapphire cell leads to a high signal-to-noise ratio and thus to the detection of phases in small quantities and light elements based compounds (LiH, MgH_2). These examples (Figure 10.a and b) also highlight the feasibility of studies involving the use of oxygen and moisture sensitive samples, such as, for example, MgH_2/Mg and $LiBH_4$, respectively.

Figure 10.c presents the structural changes of $TiVCrH_x$ additive in the kinetic study of H_2 sorption of Mg (*Courtesy of L. Laversenne, Institut Néel, Grenoble*). MgH_2-10wt%$TiVCrH_x$ composite was heated from RT to 400 °C @ 5 °C.min^{-1} under inert atmosphere (Ar) using config. A. During the heating step (patterns 1 to 150), three main phenomena were observed: 1) Narrowing of the MgH_2 diffraction peak, related to a recristallization of the compound, 2) Drift of the $TiVCrH_x$ diffraction peak position (white arrows on Figure 10.c), related to a change in the $TiVCrH_x$ lattice parameters, and 3) MgH_2 decomposition, leading to the formation of magnesium. The change in the $TiVCrH_x$ lattice parameters upon heating was attributed to a decrease of the H_2 content in $TiVCrH_x$. The rehydrogenation of the composite was performed at 380 °C under 15 bar of H_2 pressure (patterns 151

to 270). Drift of the $TiVCrH_x$ diffraction peak position, attributed to an increase of the H_2 content in $TiVCrH_x$, was observed before the formation of MgH_2. These preliminary results evidenced concomitantly changes between hydrogenation states of TiVCr and Mg. The readers might refer to the study of Laversenne *et al.* (Laversenne *et al.*, 2013) for further details and interpretations.

Figure 10.d illustrates a H_2 adsorption/desorption cycling study carried out on palladium nanoparticles confined in a carbon template (17 wt%Pd@CT, *Courtesy of C. Zlotea, ICMPE, Paris*). More details about sample synthesis can be found in (Zlotea *et al.*, 2010). The aim of this study was to monitor the change in crystallite size during cycling to highlight a nano-confinement effect. The sample (powder form) was placed in the reaction cell in config. A and the experiments were run at ambient temperature. Hydrogen adsorption was carried out under 0.1 bar of H_2 pressure whereas desorption occurred under raw vacuum (5.10^{-2} mbar). Figure 10.d represents a compilation of the Pd nanoparticles diffraction patterns over 11 adsorption/desorption cycles (noted I to XI on Figure 10.d). A cycle last 80 s (160 diffraction patterns) with 40 s under hydrogen pressure and 40 s under vacuum. The detector exposure time was fixed to 400 ms and the acquisition frequency to 2 Hz. First, these results illustrate the feasibility of adsorption/desorption cycling studies using the GLS. Second, from the FWHM of Pd(111) diffraction peak, no apparent increase in the crystallite size of Pd nanoparticles was observed after 11 cycles. However, complementary experiments are required to conclude about a possible nano-confinement effect of the carbon template.

These three examples, together with the study of the hydrogenation mechanism of $LaCuMg_8$ (Couillaud *et al.*, 2012) and the study of (Mg-Ni)-based nanoconfined hydrides synthesis (Zlotea *et al.*, 2013), illustrate the potentials of the GLS for hydrogen storage studies and for monitoring structural phase changes and in situ chemical reactions of micro and nano-sized phases at high temperature and pressure.

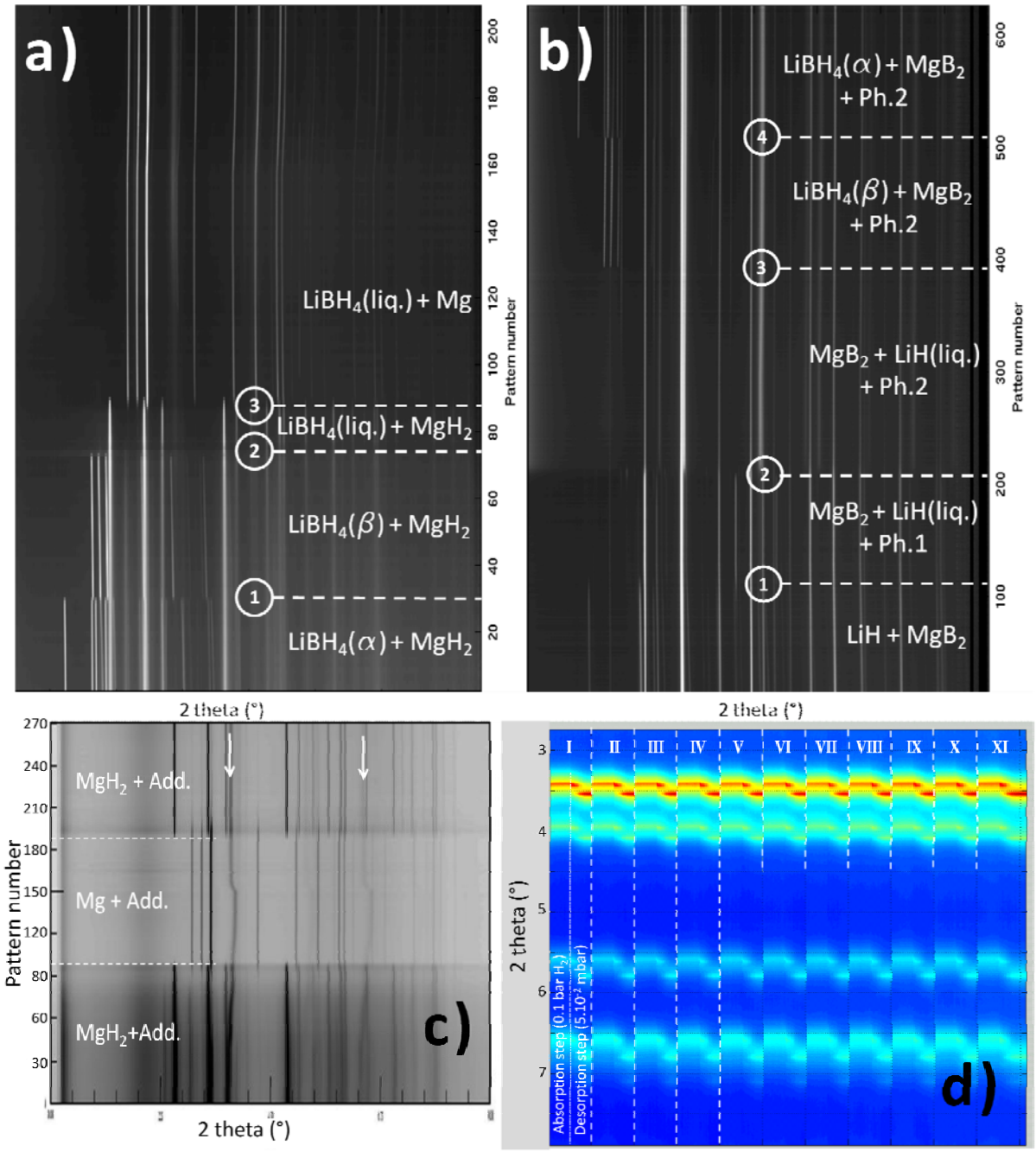

Figure 10. Illustrations of the application fields of the GLS. a) $LiBH_4$+MgH_2 RHC changes from RT to 520°C at 5°C.min^{-1} under inert atmosphere (*Courtesy of L. Laversenne, Institut Néel, Grenoble*). b) LiH-MgB_2 mixture changes during hydrogenation from 400°C to RT at 5°C.min^{-1} under 100 bar H_2 (*Courtesy of L. Laversenne, Institut Néel, Grenoble*). c) kinetics study and structural changes of $TiVCrH_x$ additive (Add., 10 wt%, white arrows) during hydrogen adsorption/desorption of magnesium (*Courtesy of L. Laversenne, Institut Néel, Grenoble*). d) cycling study of hydrogen adsorption/desorption on palladium nanoparticles confined in a carbon template (17 wt%Pd@CT) (*Courtesy of C. Zlotea, ICMPE, Paris*).

In addition to the examples described above, the authors consider two main kinds of experiments that might be performed using this new gas loading system.

The first is related to the synthesis of materials, chemicals or nanoparticles in a liquid medium and at high temperature. Given the feasibility of experiments combining liquids and solids, and the maximum working pressure of the designed cells (200 bar), solvothermal synthesis mechanisms can be studied using this system.

Second, as the system was designed to rotate (~ 200°) and translate (along y and z axes) the cell, i.e., the sample, in the X-ray beam during XRD acquisitions, XRD computed tomography (XRD-CT, Jacques *et al.* (2011)) experiments can be performed using the system. Moreover, rotation and translation of the sample are possible under high pressure and temperature, which extend the XRD-CT to XRD-CT under mild conditions. From these experiments, the phase distribution in a sample and the changes in phase distribution as a function of the time or the temperature can be determined under static pressure (using config. A) or pressurized flow of gases (using config. B). This extends the application fields of the system to the catalysis community and to studies where pressure is a major parameter influencing the reaction efficiency. Thanks to the design of a special and adjustable cell (as illustrated on Figure 1.c for example), real industrial catalyst-shaped materials, such as catalysts supported on metal foam/grid or millimeter-sized pellets, can be studied under industrial working conditions at high temperature, pressure and gas flow, i.e. under operando conditions.

5. Conclusion

This paper describes a high temperature high pressure gas loading system. This system was developed for combined in operando X-ray diffraction and mass spectrometry investigations during catalyzed gas/solid or liquid/solid reactions under high pressure and temperature. This system is based on a pressure cell, consisting of a single crystal sapphire tube, which serves both as high pressure container and reaction cell. Two different configurations of the pressure cell were developed, either under static high pressure or dynamic pressurized flow. In addition, the transportable reaction cell can be filled under an inert atmosphere inside a glove box enabling studies with oxygen/moisture sensitive compounds to be performed. Special attention was paid to the development of versatile cell designs in order to comply with specific experimental requirements and user needs. Experiments can be run in a wide working pressure range, from 10^{-3} mbar up to 200 bar, and a flow range from 0 to 1 $L.min^{-1}$ for different kinds of gases, such as H_2, N_2, Ar, CO, CO_2. Moreover, studies in a wide temperature range from 25 to 1000°C were performed using a dedicated furnace.

Acknowledgements The authors are grateful to the European Radiation Synchrotron Facility for funding and provision of beamtime for commissioning the GLS. We would like to thank Francis Bodard, Michel Garrec, Emmanuel Burtin and Isabelle Para (from ESRF Vacuum Group) and Henri Gleyzolle (ID11, ESRF) for fruitful technical discussions and developments. The authors are also grateful to L. Laversenne (Institut Néel, Grenoble) and C. Zlotea (ICMPE, Paris) for sample preparation work and the presentation of the preliminary results.

References

Arnold, M. R., Kalbitzer, H. R. & Kremer, W. (2003). *J. Magn. Reson.* **161**, 127–131.

Chupas, P. J., Chapman, K. W., Kurtz, C., Hanson, J. C., Lee, P. L. & Grey, C. P. (2008). *J. Appl. Cryst.* **41**, 822–824.

Clausen, B. S. & Topsoe, H. (1991). *Catal. Today* **9**, 189–196.

Couillaud, S., Gaudin, E., Andrieux, J., Gorsse, S., Gayot & M., Bobet, J.L. (2012). *Int. J. of Hydrogen Energy* **37**, 11824–11834.

Daniels, J. E. & Drakopoulos, M. (2009). *J. Synchrotron Rad.* **16**, 463–468.

Dobrovinskaya, E. R., Lytvynov, L. A., Pishchik, V. (2009). *Sapphire: Materials, Manufacturing, Applications*. edited by Springer Science+Business Media. New York: Springer.

Figueroa, S.J.A., Gibson D., Mairs T., Pasternak S., Newton M.A., Di Michiel M., Andrieux J., Christoforidis K.C., Iglesias-Juez A., Fernandez-Garcia M. & Prestipino C., submitted to *J. Appl. Cryst.*, Feb. 2013.

Hagen, J. (2006). *Industrial Catalysis: A Practical Approach.* 2^{d} ed., edited by Wiley-VCH Verlag GmbH & Co. KGaA. Darmstadt: betz-druck GmbH.

Hill, A.H. (2013). *J. Appl. Cryst.* **46**, 570–572.

Jacques, S. D. M., Di Michiel, M., Beale, A. M., Sochi, T., O'Brien, M. G., Espinosa-Alonso, L., Weckhuysen, B. M. & Barnes, P. (2011). *Angew. Chem. Int. Edit.* **50**, 10148–10152.

Jensen, T. R., Nielsen, T. K., Filinchuk, Y., Jørgensen, J.-E., Cerenius, Y., Gray E. MacA. & Webb, C. J. (2010). *J. Appl. Cryst.* **43**, 1456–1463.

Laversenne, L., Andrieux, J., Plante, D., Lyard, L. & Miraglia, S. (2013). *Int. J. of Hydrogen Energy* **38**, 11937–11945.

Raber, E. C., Dudley, J. A., Salerno, M. & Urayama, P. (2006). Rev. Sci. Instrum. **77**, 096106-1–3.

Spivey, J. J. & Dooley, K. M. (2010). Editors. *Catalysis*, Vol. 22. Cambridge: RSC publishing.

Wilkinson, A. P., Morelock, C. R., Greve, B. K., Jupe, A. C., Chapman, K. W., Chupas, P. J. & Kurtz C. (2010). *J. Appl. Cryst.* **44**, 1047–1053.

Zlotea, C., Cuevas, F., Paul-Boncour, V., Leroy, E., Dibandjo, P., Gadiou, R., Vix-Guterl, C. & Latroche, M. (2010). *J. Am. Chem. Soc.* **132**, 7720–7729.

Zlotea, C., Cuevas, F., Andrieux, J., Ghimbeu, C. M., Leroy, E., Léonel, E., Sengmany, Vix-Guterl, C., Gadiou, R., Martens, T. & Latroche, M. (2013). *Nano Energy* **2**, 12–20.